Journal of Hepatocellular Carcinoma

Dovepress
Taylor & Francis Group

Open Access Full Text Article

ORIGINAL RESEARCH

Development and Validation of a Machine Learning-Based Individualized Model to Predict TKI Benefit in Postoperative Recurrent HCC

Meng Li[1,2], Yumin Jiang[1], Lin Gong[2], Ruitao Sun[1], Aoyun Hao[1], Kun Liu[2], Kunye Luan[2], Zheng Jia[1], Shimei Zhang[1], Kui Liu[1], Bin Tan[1], Weiyu Hu[1], Chao Qu[1], Jingyu Cao[1]

[1]Department of Hepatobiliary and Pancreatic Surgery, Affiliated Hospital of Qingdao University, Qingdao, Shandong, People's Republic of China; [2]Department of Hepatobiliary and Pancreatic Surgery, No. 971 Hospital of the People's Liberation Army Navy, Qingdao, Shandong, People's Republic of China

Correspondence: Chao Qu; Jingyu Cao, Department of Hepatobiliary and Pancreatic Surgery, Affiliated Hospital of Qingdao University, Qingdao, Shandong, People's Republic of China, Email 201110479@bjmu.edu.cn; cjy7027@163.com

Background: Postoperative recurrence is a major contributor to poor prognosis in hepatocellular carcinoma (HCC) after curative resection. Tyrosine kinase inhibitors (TKIs) are commonly used for recurrent HCC, yet substantial interpatient heterogeneity limits their universal benefit, and reliable tools to individualize post-recurrence therapy are lacking.

Methods: We retrospectively analyzed 454 patients with recurrent HCC following curative resection. Overlap weighting based on propensity scores was applied to balance baseline characteristics between TKI-treated and non-TKI-treated groups and to assess the survival benefit of TKI therapy. Machine learning-based survival models were independently developed for each treatment cohort using multiple algorithms and internally validated. A counterfactual inference framework was implemented to estimate individualized survival outcomes under alternative treatment strategies and to identify the optimal therapy for each patient.

Results: After overlap weighting, TKI therapy was associated with improved survival compared with non-TKI treatment, including longer recurrence-free survival (median, 24 vs. 12 months; HR = 0.355, $P < 0.001$) and overall survival (median, 36 vs. 18 months; HR = 0.486, $P = 0.001$). In the non-TKI cohort, an eight-feature survival support vector machine (Surv-SVM) model achieved strong predictive performance (C-index: 0.796 in training, 0.766 in validation). In the TKI cohort, a four-feature random survival forest (RSF) model showed the highest discrimination (C-index: 0.856 and 0.838). Both models demonstrated good calibration and stable time-dependent performance. Counterfactual analysis revealed potential treatment mismatch in 23.4% of patients, including 20.7% who received non-TKI therapy but were predicted to benefit more from TKI treatment.

Conclusion: TKI therapy provides significant survival benefit in recurrent HCC after curative resection. Our machine learning-based, counterfactual framework enables individualized estimation of treatment benefit, supporting personalized post-recurrence therapy and facilitating precision management in this high-risk population.

Keywords: hepatocellular carcinoma, postoperative recurrence, tyrosine kinase inhibitor, machine learning, counterfactual reasoning

Introduction

HCC remains a leading cause of cancer-related mortality worldwide.[1] Curative resection is the primary treatment for early-stage HCC; however, postoperative recurrence is common and represents a major determinant of long-term survival.[2] Prognosis after recurrence is generally poor, making the selection of optimal post-recurrence therapy a critical and complex clinical decision.

TKIs, including sorafenib and lenvatinib, have demonstrated significant survival benefits in advanced HCC and are established as standard systemic therapies.[3–5]By targeting key pathways involved in angiogenesis and tumor proliferation, these agents delay disease progression and improve overall survival. Their efficacy has prompted increasing use in the management of recurrent HCC following curative resection. Nevertheless, evidence regarding the survival benefit of

https://doi.org/10.2147/JHC.S599142
Received: 20 February 2026
Accepted: 3 June 2026
Published: 16 June 2026

TKIs specifically in the post-recurrence setting remains inconclusive, with retrospective studies reporting inconsistent outcomes and no definitive consensus.[6,7]

Importantly, real-world data indicate that not all patients with recurrent HCC derive substantial benefit from TKI therapy.[8,9] Heterogeneity in tumor biology, liver function, and treatment tolerance contributes to variable responses. Recent studies have identified multiple molecular markers and gene signatures associated with HCC prognosis, reflecting the complex biological heterogeneity of this disease.[10,11] Consequently, indiscriminate use of TKIs may expose some patients to unnecessary toxicity and financial burden without improving survival. These observations highlight the urgent need for strategies to reliably identify individuals most likely to benefit from TKI therapy after recurrence.

A central challenge is the absence of robust predictive frameworks to guide individualized therapy selection. In current practice, post-recurrence treatment decisions are often empirical, based on physician experience or resource availability rather than evidence-based estimates of personalized benefit, which may lead to suboptimal outcomes. To address this gap, our study was designed with sequential aims: first, to evaluate the survival benefit of TKI therapy in recurrent HCC after curative resection using propensity score-based methods to control for confounding; second, to develop treatment-specific prognostic models for TKI and non-TKI cohorts employing multiple machine learning algorithms; and third, to integrate counterfactual inference to quantify individualized survival outcomes under alternative treatment strategies, thereby identifying the optimal therapeutic approach for each patient. This framework aims to provide objective, data-driven support for post-recurrence decision-making and to advance precision medicine for this high-risk population.

Material and Methods

Patients

This retrospective cohort study included patients with HCC who underwent curative resection and subsequently developed postoperative recurrence at Qingdao University Affiliated Hospital between January 2015 and December 2023.

Inclusion criteria were as follows: (1) age ≥ 18 years with no severe comorbidities or major organ dysfunction; (2) initial diagnosis of primary HCC confirmed by histopathology or non-invasive imaging criteria (multiphase CT or MRI); (3) imaging-confirmed postoperative recurrence, including local recurrence or distant metastasis; (4) availability of complete follow-up records, including detailed clinical and laboratory data; (5) receipt of TKI therapy following recurrence, with documented medication regimen, treatment duration, and response assessment.

Exclusion criteria included: (1) history of other concurrent malignancies; (2) receipt of palliative or non-radical surgery; (3) severe coagulopathy (International Normalized Ratio > 2.0) or active bleeding tendency; (4) Child-Pugh grade C liver failure or dysfunction of other vital organs; (5) loss to follow-up or interruption of planned therapy; (6) incomplete medical records precluding comprehensive analysis.

This study was conducted in accordance with the Declaration of Helsinki and approved by the Institutional Review Board of Qingdao University Affiliated Hospital. Written informed consent was obtained from all participants. Based on these criteria, a total of 454 eligible patients were included in the final analysis.

Data Collection

Baseline demographic, clinical, pathological, and laboratory data were collected. Demographic and clinical variables included age, sex, and hepatitis B virus (HBV) infection status. Primary tumor characteristics encompassed tumor size, number, histological differentiation, and the presence of microvascular or macrovascular invasion. Recurrent tumor characteristics, including the size and number of recurrent lesions, were also recorded.

Laboratory parameters included preoperative complete blood counts and liver function tests. Systemic inflammation-nutrition indices—such as neutrophil-to-lymphocyte ratio (NLR), platelet-to-lymphocyte ratio (PLR), and lymphocyte-to-monocyte ratio (LMR)—were derived from these data.

Continuous clinical variables were handled according to their distribution and clinical interpretability. Specifically, several continuous variables were categorized based on clinically meaningful thresholds and are presented as categorical

variables in Tables 1 and 2. This approach follows standard practices in clinical survival modeling and ensures consistency between model inputs and the tabulated clinical data. The primary endpoint was overall survival (OS) after recurrence, defined as the interval from the date of first confirmed recurrence to death from any cause or last follow-up. The final follow-up date was August 31, 2025.

Statistical Analysis

All statistical analyses were conducted using R software (version 4.5.0; R Foundation for Statistical Computing). Continuous variables are presented as mean ± standard deviation or median (interquartile range), and categorical variables as counts (percentages). Group comparisons were performed using Student's *t*-test, Mann–Whitney *U*-test, chi-square test, or Fisher's exact test, as appropriate. Missing data were minimal in our dataset. For variables with occasional missing values, we applied multiple imputation based on chained equations, following established protocols in previous clinical studies. This approach ensured data completeness and maintained the statistical integrity of the analyses. Variables with a ***P***-value < 0.05 were considered statistically significant.

Overlap Weighting Based on Propensity Scores Matching

To mitigate potential confounding bias, overlap weighting based on propensity scores was applied. Propensity scores, representing the probability of receiving TKI therapy, were estimated for each patient using a logistic regression model incorporating all baseline covariates. Overlap weights were then assigned to create a balanced pseudo-population.

Balance between weighted groups was assessed using standardized mean differences (SMDs), with SMD < 0.1 indicating adequate balance. Survival outcomes in the weighted cohort were compared using the weighted Kaplan-Meier method and weighted Cox proportional hazards models.

Development and Validation of Machine Learning Prognostic Models

Prognostic models were developed separately for TKI-treated and non-TKI cohorts. Although overlap weighting was applied to assess the causal effect of TKI therapy on post-recurrence outcomes, the prognostic models for individualized survival prediction were trained on the original, unweighted cohort. This approach was chosen to capture the full variability of baseline characteristics and treatment heterogeneity, and to ensure that the models can be applied to real-world patients receiving diverse post-recurrence treatments.

Feature Selection

Within a 5-fold cross-validation framework, the concordance index (C-index) was used to evaluate and compare the performance of three feature selection methods: stepwise Cox regression, RSF, and LASSO-Cox regression. The optimal feature set for each cohort was then selected.

Model Construction and Training

Using the selected features, multiple survival prediction models were constructed, including RSF, elastic net Cox regression, gradient boosting machine (GBM), and Surv-SVM. Predictive performance and stability were evaluated and compared based on the C-index distribution across cross-validation folds.

RSF model was constructed using 300 survival trees (n_estimators=300). The minimum number of samples required in terminal nodes was set to 5 (min_samples_leaf=5). At each split, the square root of the total number of variables was randomly selected as candidate features (max_features="sqrt"). Parallel computation was enabled using all available CPU cores (n_jobs=−1). Surv-SVM was performed using a regularization parameter of alpha=1×10^{-4} and a hybrid ranking–regression setting with rank_ratio=0.5. The relatively small regularization strength was selected to preserve predictive information from high-dimensional features, while the hybrid optimization strategy allowed simultaneous consideration of survival risk ranking and survival time prediction under censored survival conditions. This parameter setting was considered suitable for the characteristics of the present study, including relatively small sample size, high-dimensional feature space, and survival outcomes with censoring. Random seed was fixed at 42 to ensure reproducibility.

Table 1 Baseline Characteristics of the Targeted Therapy and Non-Targeted Therapy Groups

Variables	Total (n = 454)	TKI Group (n = 307)	Non-TKI Group (n = 147)	*P*
NEU, Mean ± SD	3.19 ± 1.46	3.22 ± 1.51	3.12 ± 1.37	0.500
MONO, Mean ± SD	0.44 ± 0.23	0.44 ± 0.25	0.45 ± 0.19	0.963
BASO, Mean ± SD	0.02 ± 0.02	0.02 ± 0.02	0.03 ± 0.04	0.201
EOS, Mean ± SD	0.12 ± 0.15	0.13 ± 0.16	0.11 ± 0.11	0.310
LYM, Mean ± SD	1.64 ± 0.64	1.68 ± 0.67	1.56 ± 0.55	**0.048**
WBC, Mean ± SD	5.41 ± 1.81	5.49 ± 1.84	5.25 ± 1.75	0.190
RBC, Mean ± SD	4.66 ± 0.57	4.66 ± 0.55	4.65 ± 0.60	0.941
HGB, Mean ± SD	144.39 ± 17.85	144.44 ± 16.97	144.29 ± 19.62	0.933
PLT, Mean ± SD	159.01 ± 62.57	157.70 ± 58.80	161.74 ± 69.92	0.521
ALB, Mean ± SD	42.33 ± 5.80	42.63 ± 5.71	41.69 ± 5.97	0.108
TBIL, Mean ± SD	19.94 ± 17.05	19.13 ± 8.85	21.66 ± 27.08	0.139
DBIL, Mean ± SD	7.09 ± 12.11	6.36 ± 2.73	8.59 ± 20.89	0.067
ALP, Mean ± SD	84.16 ± 40.94	83.33 ± 39.64	85.89 ± 43.62	0.534
IBIL, Mean ± SD	12.68 ± 6.69	12.48 ± 5.94	13.11 ± 8.04	0.351
ALT, Mean ± SD	41.53 ± 51.00	37.73 ± 28.39	49.50 ± 79.45	**0.084**
AST, Mean ± SD	36.31 ± 40.69	33.53 ± 22.65	42.10 ± 63.33	0.113
GGT, Mean ± SD	70.36 ± 100.32	67.47 ± 105.16	76.39 ± 89.43	0.376
NER, Mean ± SD	61.37 ± 107.14	62.33 ± 118.75	59.35 ± 77.79	0.782
NLR, Mean ± SD	2.31 ± 2.18	2.37 ± 2.51	2.21 ± 1.26	0.480
PLR, Mean ± SD	108.10 ± 59.30	106.54 ± 59.78	111.36 ± 58.35	0.419
LMR, Mean ± SD	4.19 ± 1.84	4.34 ± 1.83	3.89 ± 1.82	**0.015**
Gender, n(%)				0.514
Female	67 (14.76)	43 (14.01)	24 (16.33)	
Male	387 (85.24)	264 (85.99)	123 (83.67)	
Age at surgery, n(%)				0.534
<60 years	253 (55.73)	168 (54.72)	85 (57.82)	
≥60 years	201 (44.27)	139 (45.28)	62 (42.18)	
Preoperative Intervention, n(%)				**<0.001**
No	137 (30.18)	38 (12.38)	99 (67.35)	
Yes	317 (69.82)	269 (87.62)	48 (32.65)	
HBV, n(%)				**<0.001**
No	325 (71.59)	289 (94.14)	36 (24.49)	
Yes	129 (28.41)	18 (5.86)	111 (75.51)	
Pre-AFP, n(%)				0.104
<7 ng/mL	119 (26.33)	87 (28.52)	32 (21.77)	
7–400 ng/mL	189 (41.81)	130 (42.62)	59 (40.14)	
>400 ng/mL	144 (31.86)	88 (28.85)	56 (38.10)	
Pre-MDT, n(%)				**0.014**
<5 cm	269 (59.25)	194 (63.19)	75 (51.02)	
≥5 cm	185 (40.75)	113 (36.81)	72 (48.98)	
Pre-NT, n(%)				0.794
1	398 (87.67)	271 (88.27)	127 (86.39)	
2	48 (10.57)	31 (10.10)	17 (11.56)	
≥3	8 (1.76)	5 (1.63)	3 (2.04)	
Degree of differentiation, n(%)				**0.009**
Poorly	235 (51.76)	172 (56.03)	63 (42.86)	
Moderately to highly	219 (48.24)	135 (43.97)	84 (57.14)	
MVI, n(%)				0.195
0	210 (46.26)	149 (48.53)	61 (41.50)	
1	167 (36.78)	112 (36.48)	55 (37.41)	
2	77 (16.96)	46 (14.98)	31 (21.09)	
Bile duct invasion and cancer thrombus, n(%)				0.540
No	443 (97.58)	301 (98.05)	142 (96.60)	
Yes	11 (2.42)	6 (1.95)	5 (3.40)	

(*Continued*)

Table 1 (Continued).

Variables	Total (n = 454)	TKI Group (n = 307)	Non-TKI Group (n = 147)	*P*
Liver capsule, n(%)				0.257
No	242 (53.30)	158 (51.47)	84 (57.14)	
Yes	212 (46.70)	149 (48.53)	63 (42.86)	
Satellite nodules, n(%)				0.782
No	386 (85.02)	262 (85.34)	124 (84.35)	
Yes	68 (14.98)	45 (14.66)	23 (15.65)	
Nerve invasion, n(%)				0.438
No	441 (97.14)	300 (97.72)	141 (95.92)	
Yes	13 (2.86)	7 (2.28)	6 (4.08)	
Cirrhosis, n(%)				0.963
No	163 (35.90)	110 (35.83)	53 (36.05)	
Yes	291 (64.10)	197 (64.17)	94 (63.95)	
Postoperative intervention, n(%)				0.298
No	269 (59.25)	187 (60.91)	82 (55.78)	
Yes	185 (40.75)	120 (39.09)	65 (44.22)	
First recurrence site, n(%)				**<0.001**
Extrahepatic	49 (10.79)	20 (6.51)	29 (19.73)	
Intrahepatic	392 (86.34)	280 (91.21)	112 (76.19)	
Both	13 (2.86)	7 (2.28)	6 (4.08)	
Maximum diameter of tumor at recurrence, n(%)				0.799
<3cm	256 (56.64)	174 (57.05)	82 (55.78)	
≥3 cm	196 (43.36)	131 (42.95)	65 (44.22)	
Number of tumor at recurrence, n(%)				0.336
1	217 (47.80)	154 (50.16)	63 (42.86)	
2	35 (7.71)	22 (7.17)	13 (8.84)	
≥ 3	202 (44.49)	131 (42.67)	71 (48.30)	
AFP at recurrence, n(%)				**0.090**
<7 ng/mL	174 (39.19)	127 (42.76)	47 (31.97)	
7–400 ng/mL	183 (41.22)	115 (38.72)	68 (46.26)	
>400 ng/mL	87 (19.59)	55 (18.52)	32 (21.77)	
Interventional treatment after recurrence, n(%)				0.161
No	150 (33.04)	108 (35.18)	42 (28.57)	
Yes	304 (66.96)	199 (64.82)	105 (71.43)	
Surgery treatment after recurrence, n(%)				0.321
No	266 (58.59)	175 (57.00)	91 (61.90)	
Yes	188 (41.41)	132 (43.00)	56 (38.10)	

Notes: Bold values indicate statistically significant differences (***P*** < 0.05).

Abbreviations: NEU, neutrophil count; MONO, monocyte count; BASO, basophil count; EOS, eosinophil count; LYM, lymphocyte count; WBC, white blood cell count; RBC, red blood cell count; HGB, hemoglobin; PLT, platelet count; ALB, albumin; TBIL, total bilirubin; DBIL, direct bilirubin; ALP, alkaline phosphatase; IBIL, indirect bilirubin; ALT, alanine aminotransferase; AST, aspartate aminotransferase; GGT, gamma-glutamyl transferase; NER, neutrophil-to-erythrocyte ratio; NLR, neutrophil-to-lymphocyte ratio; PLR, platelet-to-lymphocyte ratio; LMR, lymphocyte-to-monocyte ratio; HBV, hepatitis B virus; Pre-AFP, preoperative alpha-fetoprotein; Pre-MDT, preoperative maximum tumor diameter; Pre-NT, preoperative number of tumors; MVI, microvascular invasion.

Model Evaluation

Validated models were assessed using multiple approaches: (1) risk stratification ability via Kaplan-Meier analysis with Log rank test; (2) predictive discrimination over time using time-dependent area under the receiver operating characteristic curve (AUC); (3) prediction accuracy measured by time-dependent Brier scores and calibration curves; (4) feature importance interpreted at the individual level using SHapley Additive exPlanations (SHAP).

Counterfactual Framework for Treatment Strategy Matching Analysis

A counterfactual prediction framework was implemented to analyze personalized treatment matching. For each patient, the two validated cohort-specific models were used to predict 24-month recurrence risk under two counterfactual

Table 2 Baseline Characteristics Before and After Propensity Score Overlap Weighting

Variable	Before PSM				After PSM			
	Non-TKI Group (n = 307)	TKI Group (n = 147)	*P*	SMD	Non- TKI Group (n = 105)	TKI Group (n = 54)	*P*	SMD
NEU, Mean ± SD	3.22 ± 1.51	3.12 ± 1.37	0.500	−0.072	3.05 ± 1.36	3.02 ± 1.38	0.896	−0.022
MONO, Mean ± SD	0.44 ± 0.25	0.45 ± 0.19	0.963	0.006	0.41 ± 0.24	0.41 ± 0.18	0.830	0.045
BASO, Mean ± SD	0.02 ± 0.02	0.03 ± 0.04	0.201	0.088	0.02 ± 0.02	0.03 ± 0.05	0.464	0.079
EOS, Mean ± SD	0.13 ± 0.16	0.11 ± 0.11	0.310	−0.135	0.11 ± 0.08	0.11 ± 0.09	0.996	0.001
LYM, Mean ± SD	1.68 ± 0.67	1.56 ± 0.55	**0.048**	−0.229	1.47 ± 0.54	1.50 ± 0.52	0.750	0.055
WBC, Mean ± SD	5.49 ± 1.84	5.25 ± 1.75	0.190	−0.137	5.06 ± 1.68	5.07 ± 1.74	0.989	0.002
RBC, Mean ± SD	4.66 ± 0.55	4.65 ± 0.60	0.941	−0.007	4.72 ± 0.52	4.70 ± 0.62	0.825	−0.033
HGB, Mean ± SD	144.44 ± 16.97	144.29 ± 19.62	0.933	−0.008	144.46 ± 18.32	145.41 ± 21.12	0.769	0.045
PLT, Mean ± SD	157.70 ± 58.80	161.74 ± 69.92	0.521	0.058	151.40 ± 62.97	154.07 ± 68.57	0.806	0.039
ALB, Mean ± SD	42.63 ± 5.71	41.69 ± 5.97	0.108	−0.158	42.88 ± 5.85	42.99 ± 6.08	0.909	0.019
TBIL,Mean ± SD	19.13 ± 8.85	21.66 ± 27.08	0.139	0.093	20.01 ± 7.75	21.96 ± 30.43	0.535	0.064
DBIL,Mean ± SD	6.36 ± 2.73	8.59 ± 20.89	0.067	0.107	6.84 ± 2.96	8.71 ± 21.14	0.374	0.088
ALP, Mean ± SD	83.33 ± 39.64	85.89 ± 43.62	0.534	0.059	87.03 ± 41.25	80.60 ± 34.71	0.329	−0.185
IBIL,Mean ± SD	12.48 ± 5.94	13.11 ± 8.04	0.351	0.078	13.33 ± 5.53	13.37 ± 10.09	0.972	0.004
ALT, Mean ± SD	37.73 ± 28.39	49.50 ± 79.45	0.084	0.148	36.93 ± 25.72	49.47 ± 106.40	0.253	0.118
AST, Mean ± SD	33.53 ± 22.65	42.10 ± 63.33	0.113	0.135	33.61 ± 17.02	43.17 ± 96.04	0.322	0.100
GGT, Mean ± SD	67.47 ± 105.16	76.39 ± 89.43	0.376	0.100	73.58 ± 80.88	73.08 ± 85.82	0.971	−0.006
NER, Mean ± SD	62.33 ± 118.75	59.35 ± 77.79	0.782	−0.038	54.72 ± 61.64	53.39 ± 71.48	0.904	−0.018
NLR, Mean ± SD	2.37 ± 2.51	2.21 ± 1.26	0.480	−0.122	2.31 ± 1.29	2.17 ± 1.16	0.501	−0.121
PLR, Mean ± SD	106.54 ± 59.78	111.36 ± 58.35	0.419	0.083	110.44 ± 49.93	106.93 ± 41.22	0.657	−0.085
LMR, Mean ± SD	4.34 ± 1.83	3.89 ± 1.82	0.015	−0.246	4.27 ± 1.98	4.03 ± 1.79	0.461	−0.133
Gender, n (%)			0.514				0.713	
Female	43 (14.01)	24 (16.33)		0.063	20 (19.05)	9 (16.67)		−0.064
Male	264 (85.99)	123 (83.67)		−0.063	85 (80.95)	45 (83.33)		0.064
Age at surgery, n (%)			0.534				0.975	
<60 years	168 (54.72)	85 (57.82)		0.063	60 (57.14)	31 (57.41)		0.005
≥60 years	139 (45.28)	62 (42.18)		−0.063	45 (42.86)	23 (42.59)		−0.005
Preoperative Intervention, n (%)			**<0.001**				0.003	
No	38 (12.38)	99 (67.35)		1.172	28 (26.67)	27 (50.00)		0.467
Yes	269 (87.62)	48 (32.65)		−1.172	77 (73.33)	27 (50.00)		−0.467
HBV, n (%)			**<0.001**				0.001	
No	289 (94.14)	36 (24.49)		−1.620	87 (82.86)	32 (59.26)		−0.480
Yes	18 (5.86)	111 (75.51)		1.620	18 (17.14)	22 (40.74)		0.480
Pre-AFP, n (%)			0.104				0.487	
<7 ng/mL	87 (28.52)	32 (21.77)		−0.164	25 (23.81)	14 (25.93)		0.048
7–400 ng/mL	130 (42.62)	59 (40.14)		−0.051	41 (39.05)	25 (46.30)		0.145
>400 ng/mL	88 (28.85)	56 (38.10)		0.190	39 (37.14)	15 (27.78)		−0.209

https://doi.org/10.2147/JHC.S599142

Pre-MDT, n (%)			**0.014**				0.201	
<5 cm	194 (63.19)	75 (51.02)		−0.243	51 (48.57)	32 (59.26)		0.218
≥5 cm	113 (36.81)	72 (48.98)		0.243	54 (51.43)	22 (40.74)		−0.218
Pre-NT, n (%)			0.794				0.518	
1	271 (88.27)	127 (86.39)		−0.055	89 (84.76)	50 (92.59)		0.299
2	31 (10.10)	17 (11.56)		0.046	13 (12.38)	3 (5.56)		−0.298
3	5 (1.63)	3 (2.04)		0.052	2 (1.90)	1 (1.85)		−0.004
Degree of differentiation, n (%)			**0.009**				0.975	
Poorly	172 (56.03)	63 (42.86)		−0.266	45 (42.86)	23 (42.59)		−0.005
Moderately to highly	135 (43.97)	84 (57.14)		0.266	60 (57.14)	31 (57.41)		0.005
MVI, n (%)			0.195				0.990	
0	149 (48.53)	61 (41.50)		−0.143	44 (41.90)	22 (40.74)		−0.024
1	112 (36.48)	55 (37.41)		0.019	42 (40.00)	22 (40.74)		0.015
2	46 (14.98)	31 (21.09)		0.150	19 (18.10)	10 (18.52)		0.011
Bile duct invasion and cancer thrombus, n (%)			0.540				0.554	
No	301 (98.05)	142 (96.60)		−0.080	104 (99.05)	52 (96.30)		−0.146
Yes	6 (1.95)	5 (3.40)		0.080	1 (0.95)	2 (3.70)		0.146
Liver capsule, n (%)			0.257				0.628	
No	158 (51.47)	84 (57.14)		0.115	58 (55.24)	32 (59.26)		0.082
Yes	149 (48.53)	63 (42.86)		−0.115	47 (44.76)	22 (40.74)		−0.082
Satellite nodules, n(%)			0.782				0.270	
No	262 (85.34)	124 (84.35)		−0.027	84 (80.00)	47 (87.04)		0.210
Yes	45 (14.66)	23 (15.65)		0.027	21 (20.00)	7 (12.96)		−0.210
Nerve invasion, n (%)			0.438				0.549	
No	300 (97.72)	141 (95.92)		−0.091	103 (98.10)	54 (100.00)		0.171
Yes	7 (2.28)	6 (4.08)		0.091	2 (1.90)	0 (0.00)		−0.171
Cirrhosis, n (%)			0.963				0.159	
No	110 (35.83)	53 (36.05)		0.005	41 (39.05)	15 (27.78)		−0.252
Yes	197 (64.17)	94 (63.95)		−0.005	64 (60.95)	39 (72.22)		0.252
Postoperative intervention, n (%)			0.298				0.356	
No	187 (60.91)	82 (55.78)		−0.103	70 (66.67)	32 (59.26)		−0.151
Yes	120 (39.09)	65 (44.22)		0.103	35 (33.33)	22 (40.74)		0.151
First recurrence site, n(%)			**<0.001**				0.745	
Extrahepatic	20 (6.51)	29 (19.73)		0.332	12 (11.43)	8 (14.81)		0.095
Intrahepatic	280 (91.21)	112 (76.19)		−0.353	89 (84.76)	45 (83.33)		−0.038
Both	7 (2.28)	6 (4.08)		0.091	4 (3.81)	1 (1.85)		−0.145
Maximum diameter of tumor at recurrence, n (%)			0.799				0.808	
<3cm	174 (57.05)	82 (55.78)		−0.026	66 (62.86)	35 (64.81)		0.041
≥3 cm	131 (42.95)	65 (44.22)		0.026	39 (37.14)	19 (35.19)		−0.041

(*Continued*)

https://doi.org/10.2147/JHC.S599142

Table 2 (Continued).

Variable	Before PSM				After PSM			
	Non-TKI Group (n = 307)	TKI Group (n = 147)	*P*	SMD	Non- TKI Group (n = 105)	TKI Group (n = 54)	*P*	SMD
Number of tumor at recurrence, n (%)			0.336				0.954	
1	154 (50.16)	63 (42.86)		−0.148	44 (41.90)	24 (44.44)		0.051
2	22 (7.17)	13 (8.84)		0.059	10 (9.52)	5 (9.26)		−0.009
≥ 3	131 (42.67)	71 (48.30)		0.113	51 (48.57)	25 (46.30)		−0.046
AFP at recurrence, n(%)			0.090				0.442	
<7 ng/mL	127 (42.76)	47 (31.97)		−0.231	33 (31.43)	22 (40.74)		0.190
7–400 ng/mL	115 (38.72)	68 (46.26)		0.151	51 (48.57)	21 (38.89)		−0.199
>400 ng/mL	55 (18.52)	32 (21.77)		0.079	21 (20.00)	11 (20.37)		0.009
Interventional treatment after recurrence, n (%)			0.161				0.873	
No	108 (35.18)	42 (28.57)		−0.146	26 (24.76)	14 (25.93)		0.027
Yes	199 (64.82)	105 (71.43)		0.146	79 (75.24)	40 (74.07)		−0.027
Surgery treatment after recurrence, n (%)			0.321				0.823	
No	175 (57.00)	91 (61.90)		0.101	68 (64.76)	34 (62.96)		−0.037
Yes	132 (43.00)	56 (38.10)		−0.101	37 (35.24)	20 (37.04)		0.037

Notes: Bold values indicate statistically significant differences (***P*** < 0.05).

Abbreviations: NEU, neutrophil count; MONO, monocyte count; BASO, basophil count; EOS, eosinophil count; LYM, lymphocyte count; WBC, white blood cell count; RBC, red blood cell count; HGB, hemoglobin; PLT, platelet count; ALB, albumin; TBIL, total bilirubin; DBIL, direct bilirubin; ALP, alkaline phosphatase; IBIL, indirect bilirubin; ALT, alanine aminotransferase; AST, aspartate aminotransferase; GGT, gamma-glutamyl transferase; NER, neutrophil-to-erythrocyte ratio; NLR, neutrophil-to-lymphocyte ratio; PLR, platelet-to-lymphocyte ratio; LMR, lymphocyte-to-monocyte ratio; HBV, hepatitis B virus; Pre-AFP, preoperative alpha-fetoprotein; Pre-MDT, preoperative maximum tumor diameter; Pre-NT, preoperative number of tumors; MVI, microvascular invasion.

https://doi.org/10.2147/JHC.S599142

scenarios: receiving TKI therapy or not. The absolute difference in predicted risk between scenarios was calculated, with a risk difference > 0.05 predefined as clinically significant for treatment recommendation.[12]

Patients were subsequently classified into four decision quadrants based on actual treatment received versus model-recommended treatment (lower predicted risk). This analysis quantified alignment between real-world treatment and model-based recommendations, identifying potential mismatches and providing evidence for individualized clinical decision-making.

Results

Baseline Characteristics of the Study Cohort

A total of 454 patients with recurrent HCC treated at Qingdao University Affiliated Hospital between January 2015 and December 2023 were included (Figure 1). The cohort comprised 387 males (85.2%), and 253 patients (55.7%) were younger than 60 years at the time of surgery. Based on post-recurrence treatment, patients were categorized into a non-TKI group (n = 307) and a TKI therapy group (n = 147). Detailed baseline characteristics are summarized in Table 1. Intergroup comparisons revealed significant differences in lymphocyte count ($P = 0.048$), LMR ($P = 0.015$), history of preoperative interventional therapy, HBV infection status, maximum preoperative tumor diameter, tumor differentiation, and site of first recurrence (all $P < 0.05$). Other variables showed no significant differences (all $P > 0.05$).

Survival Outcomes After Overlap Weighting Adjustment

After applying overlap weighting, propensity score distributions were well-balanced, resulting in a weighted cohort of 54 patients in the TKI therapy group and 105 in the non- TKI group (approximately 1:2 ratio). Covariate balance assessment (Table 2) confirmed that previously imbalanced variables were adequately balanced after weighting (all $P > 0.05$). Overlapping probability density curves (Figure 2A) and standardized mean differences below 0.1 for all covariates (Figure 2B) demonstrated successful covariate adjustment.

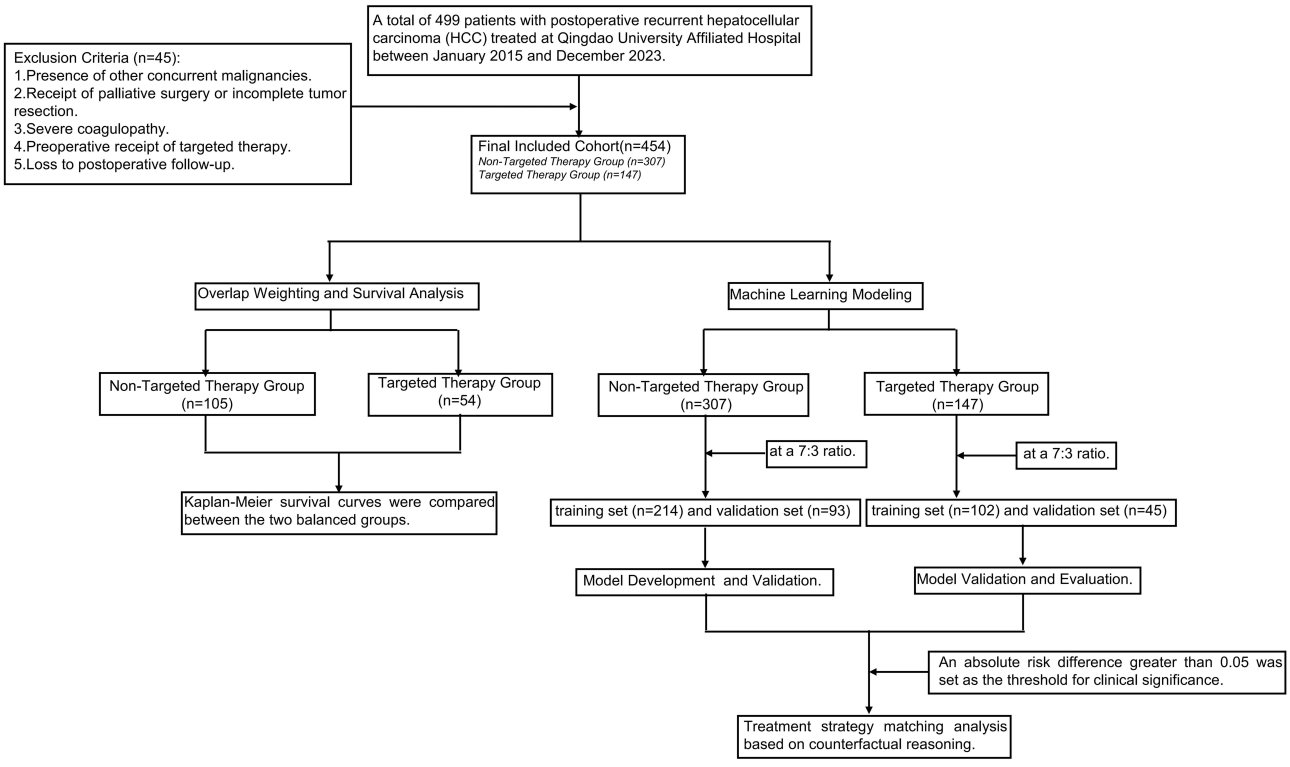

Figure 1 Flowchart of patient selection, matching, and modeling procedures.

https://doi.org/10.2147/JHC.S599142

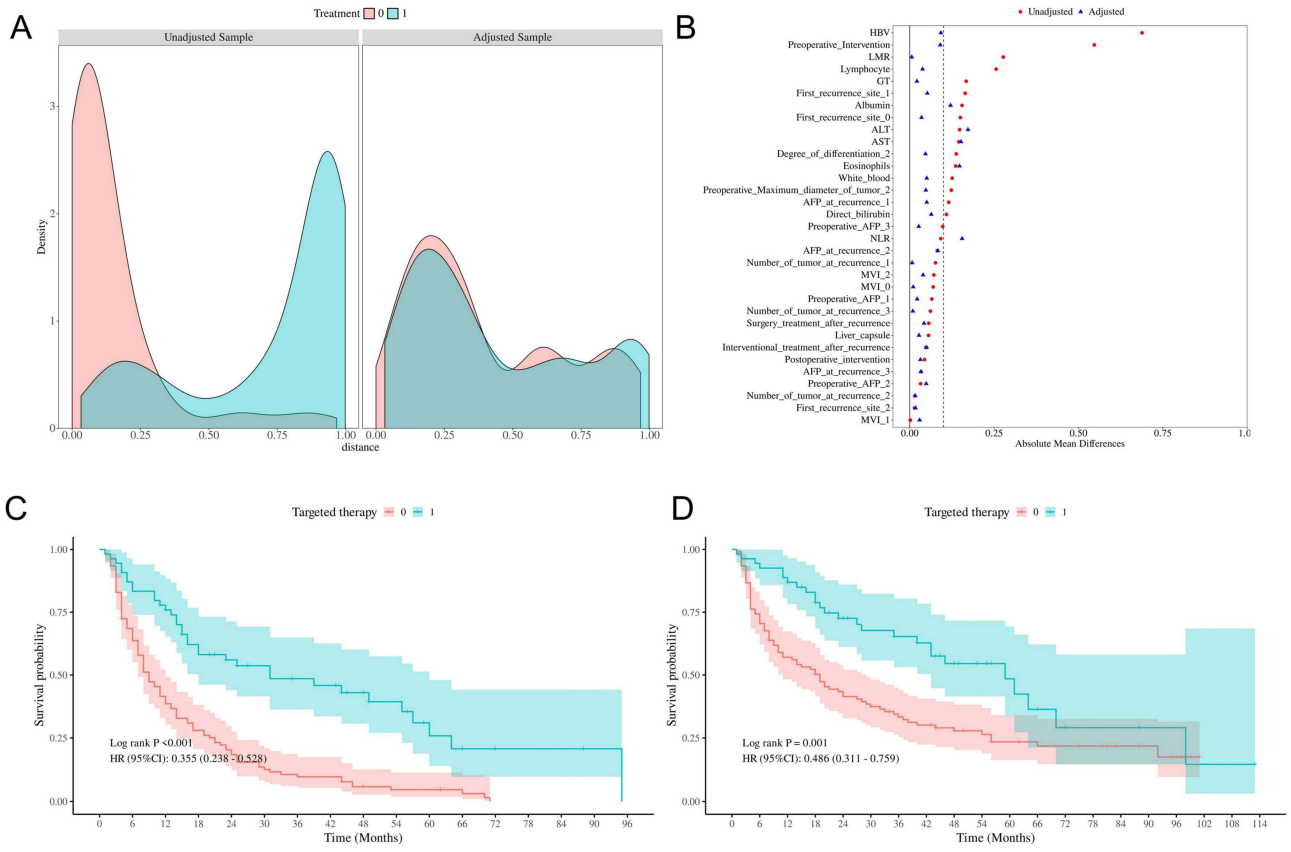

Figure 2 Evaluation of cohort balance and survival outcomes after propensity score overlap weighting. (**A**) Density distribution of propensity scores in the TKI-TKI therapy and non-TKI therapy groups after weighting. (**B**) Standardized mean differences (SMD) for all baseline covariates between the TKI-TKI therapy and non-TKI therapy groups after weighting. (**C**) Kaplan–Meier curves for recurrence-free survival (RFS) in the TKI-TKI therapy and non-TKI therapy groups. (**D**) Kaplan–Meier curves for overall survival (OS) in the TKI-TKI therapy and non-TKI therapy groups.

Survival analysis showed significantly improved outcomes in the TKI therapy group. Median recurrence-free survival (RFS) was 24 months versus 12 months in the non-targeted group (HR = 0.355; 95% CI: 0.238–0.528; $\boldsymbol{P} < 0.001$; Figure 2C). Median OS was 36 months versus 18 months (HR = 0.486; 95% CI: 0.311–0.759; $\boldsymbol{P} = 0.001$; Figure 2D), indicating that, after adjustment for confounding, TKI therapy significantly prolongs both RFS and OS.

Prognostic Model for the Non- TKI Subgroup

Feature Selection

Patients in the non-TKI group were randomly split into training (n = 214) and validation (n = 93) sets in a 7:3 ratio. The results of univariate and multivariate Cox regression analyses for the non-TKI subgroups are summarized in Table 3. Among stepwise Cox regression, RSF, and LASSO-Cox methods, stepwise Cox regression yielded the optimal eight-feature set: surgery/ablation after recurrence, number of recurrent tumors, interventional therapy after recurrence, maximum preoperative tumor diameter, AFP level at recurrence, satellite nodules, HBV infection status, and nerve invasion.

Algorithm Comparison and Model Construction

Using this feature set, four algorithms—RSF, Elastic Net Cox, GBM, and Surv-SVM —were compared (Figure 3A). Five-fold cross-validation (Figure 3B) identified Surv-SVM as having the highest and most stable median C-index (0.79). Comprehensive evaluation (Figure 3C) confirmed its superior average C-index (0.783) and 24-month time-dependent AUC (0.875), establishing it as the final model. Feature importance ranking (Figure 3D) highlighted surgery/ablation after recurrence, number of recurrent tumors, and interventional therapy after recurrence as the top predictors.

Table 3 Univariate and Multivariate Cox Regression Analyses of Clinical Factors Associated with Recurrence in No Targeted Therapy Patients with HCC

Characteristic	Univariate HR (95% CI)	*P*	Multivariate HR (95% CI)	*P*
Surgery	0.526 (0.455–0.607)	**<0.001**	0.575 (0.490–0.673)	**<0.001**
NT	1.820 (1.589–2.085)	**<0.001**	1.657 (1.426–1.924)	**<0.001**
Pre-MDT	1.459 (1.283–1.659)	**<0.001**	1.239 (1.082–1.418)	**0.002**
Satellite nodules	1.311 (1.162–1.480)	**<0.001**	1.186 (1.043–1.349)	**0.009**
Degree of differentiation	1.342 (1.177–1.531)	**<0.001**		
MVI	1.326 (1.169–1.504)	**<0.001**		
MDT	1.296 (1.138–1.476)	**<0.001**		
AFP	1.300 (1.138–1.485)	**<0.001**	1.185 (1.035–1.357)	**0.014**
GGT	1.268 (1.122–1.433)	**<0.001**		
HBV	0.702 (0.570–0.865)	**<0.001**	0.780 (0.632–0.962)	**0.020**
Nerve invasion	1.203 (1.074–1.348)	**0.001**	1.199 (1.069–1.344)	**0.002**
Bile duct invasion and cancer thrombus	1.197 (1.069–1.341)	**0.002**		
ALP	1.210 (1.068–1.370)	**0.003**		
Pre-AFP	1.191 (1.045–1.359)	**0.009**		
Invention	0.848 (0.744–0.966)	**0.013**	0.631 (0.547–0.727)	**<0.001**
EOS	1.150 (1.030–1.284)	**0.013**		
Pre-Intervention	1.178 (1.019–1.363)	**0.027**		
PLR	1.124 (1.010–1.251)	**0.033**		
Liver capsule	1.150 (1.008–1.311)	**0.038**		
PLT	1.127 (0.983–1.292)	0.087		
HGB	0.908 (0.802–1.027)	0.125		
Pre-NT	1.109 (0.970–1.269)	0.131		
First recurrence site	0.897 (0.769–1.046)	0.165		
NER	0.917 (0.793–1.061)	0.243		
LMR	0.930 (0.809–1.068)	0.303		
Age at surgery	1.063 (0.933–1.212)	0.358		
NLR	1.052 (0.941–1.177)	0.374		
DBIL	1.061 (0.929–1.212)	0.383		
AST	1.043 (0.945–1.150)	0.406		
LYM	0.944 (0.821–1.085)	0.416		
ALB	1.043 (0.908–1.197)	0.555		
TBIL	1.038 (0.915–1.178)	0.558		
MONO	1.041 (0.905–1.197)	0.576		
Gender	1.039 (0.907–1.189)	0.585		
IBIL	1.014 (0.897–1.146)	0.824		
RBC	1.012 (0.889–1.151)	0.858		
Cirrhosis	0.991 (0.870–1.128)	0.887		
NEU	1.008 (0.891–1.141)	0.896		
BASO	1.003 (0.880–1.142)	0.968		
ALT	1.001 (0.886–1.132)	0.981		
WBC	1.000 (0.880–1.135)	0.996		

Notes: Bold values indicate statistically significant differences ($P < 0.05$).

Abbreviations: NT, number of tumors; Pre-MDT, preoperative maximum tumor diameter; MVI, microvascular invasion; MDT, maximum tumor diameter; AFP, alpha-fetoprotein; GGT, gamma-glutamyl transferase; HBV, hepatitis B virus; ALP, alkaline phosphatase; Pre-AFP, preoperative alpha-fetoprotein; EOS, eosinophil count; Pre-intervention, preoperative intervention; PLR, platelet-to-lymphocyte ratio; PLT, platelet count; HGB, hemoglobin; Pre-NT, preoperative number of tumors; NER, neutrophil-to-erythrocyte ratio; LMR, lymphocyte-to-monocyte ratio; NLR, neutrophil-to-lymphocyte ratio; DBIL, direct bilirubin; AST, aspartate aminotransferase; LYM, lymphocyte count; ALB, albumin; TBIL, total bilirubin; MONO, monocyte count; IBIL, indirect bilirubin; RBC, red blood cell count; NEU, neutrophil count; BASO, basophil count; ALT, alanine aminotransferase; WBC, white blood cell count.

https://doi.org/10.2147/JHC.S599142

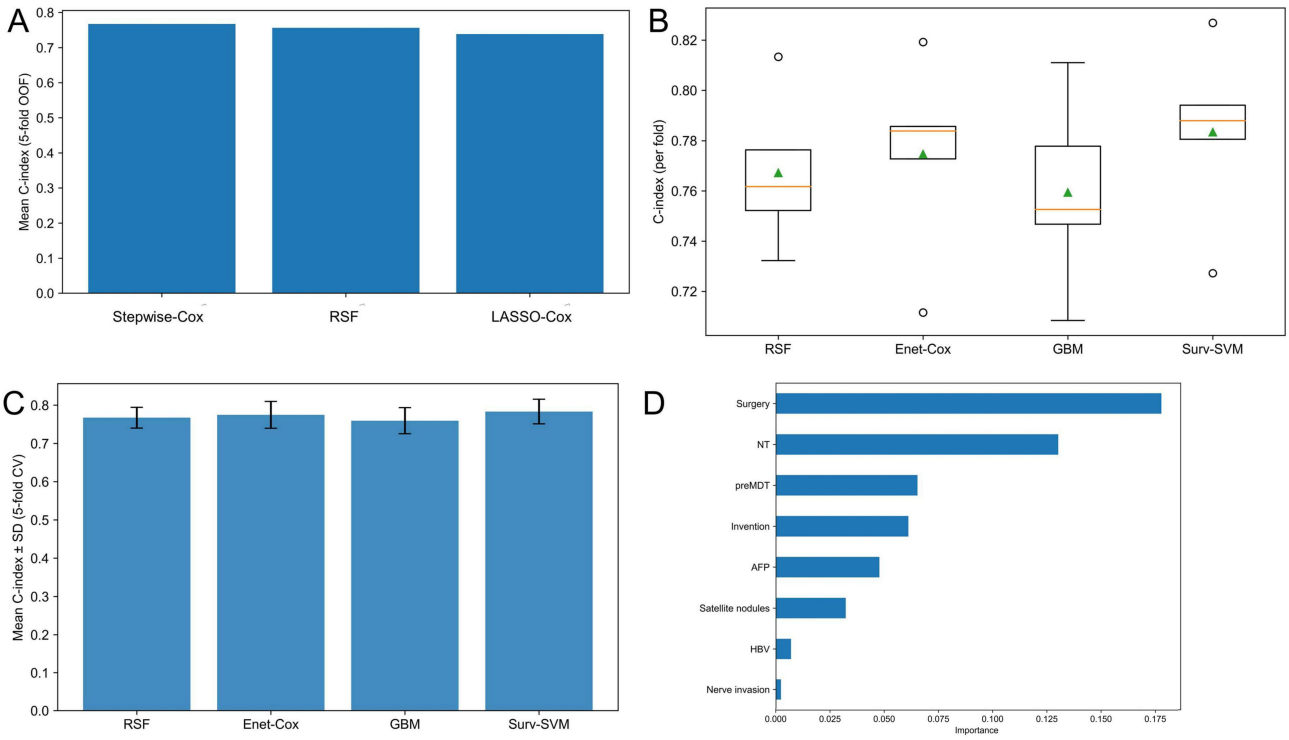

Figure 3 Development and evaluation of the prognostic prediction model for the non-TKI therapy cohort. (**A**) Comparison of three feature selection methods: stepwise Cox regression, random survival forest (RSF), and LASSO-Cox regression. (**B**) Distribution of the concordance index (C-index) across five-fold cross-validation for the four candidate prediction algorithms. (**C**) Performance comparison of the four machine learning algorithms based on comprehensive evaluation metrics. (**D**) Ranking of the importance of the selected predictive features in the final model.

Model Validation and Evaluation

Kaplan-Meier survival analysis (Figure 4A and B) demonstrated significant OS separation between low- and high-risk groups in both training (C-index = 0.796, $P < 0.001$) and validation sets (C-index = 0.766, $P < 0.001$). Time-dependent AUC remained above 0.82 throughout the 70-month follow-up (Figure 4C), indicating stable discrimination. Time-dependent Brier scores (Figure 4D) suggested optimal calibration during mid-follow-up, with overlapping curves for training and validation sets. The 24-month calibration curve (Figure 4E and F) further validated predictive accuracy. SHAP analysis (Figure 4G) identified surgery/ablation or interventional therapy post-recurrence as the strongest protective factors, whereas an increased number of recurrent tumors was the primary risk factor.

Prognostic Model for the TKI Therapy Subgroup

Feature Selection

The TKI therapy cohort was split into training (n = 102) and validation (n = 45) sets in a 7:3 ratio. The results of univariate and multivariate Cox regression analyses for the TKI therapy subgroups are summarized in Table 4. Stepwise Cox regression, RSF, and LASSO-Cox methods were used for feature selection. RSF identified four key predictors: maximum tumor diameter at recurrence, surgery/ablation after recurrence, platelet count, and number of recurrent tumors (Figure 5A).

Algorithm Comparison and Model Construction

Model comparison using these variables in five-fold cross-validation (Figure 5B and C) identified RSF as the optimal model, demonstrating superior predictive discrimination (average C-index: 0.778), stability, and 24-month time-dependent AUC (0.851). Feature importance ranking (Figure 5D) indicated maximum tumor diameter at recurrence as the most critical predictor, followed by platelet count and surgery/ablation after recurrence.

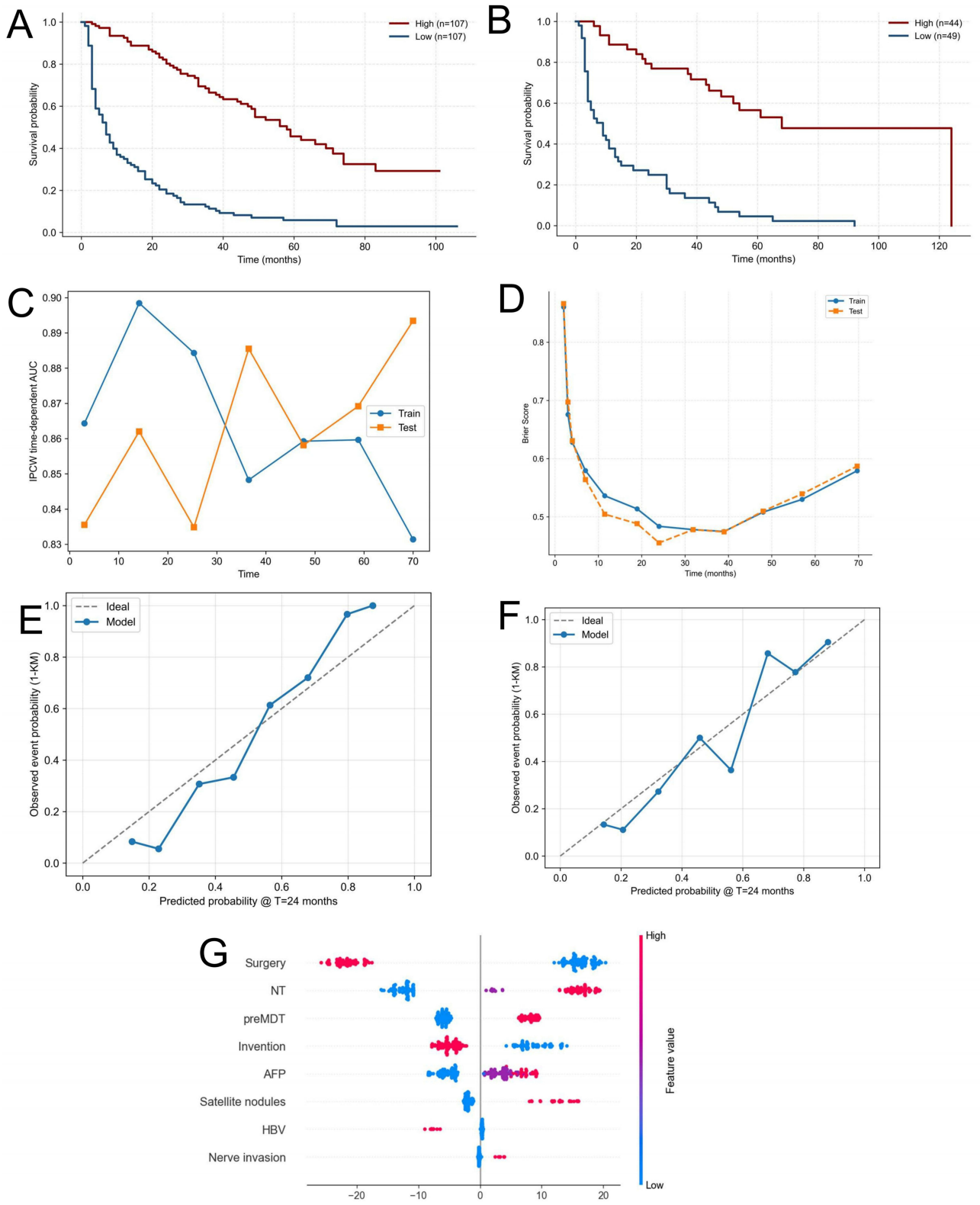

Figure 4 Validation and interpretation of the prognostic model for the non-TKI therapy cohort. (**A**) Kaplan-Meier overall survival (OS) curves for the low- and high-risk groups in the training set. (**B**) Kaplan-Meier overall survival (OS) curves for the low- and high-risk groups in the validation set. (**C**) Time-dependent area under the curve (AUC) for the model over the 70-month follow-up period. (**D**) Time-dependent Brier score for assessing the calibration of the model. (**E-F**) Calibration plots comparing predicted and observed survival probability at 24 months. (**G**) SHapley Additive exPlanations (SHAP) summary plot showing the impact of key features on model output.

https://doi.org/10.2147/JHC.S599142

Table 4 Univariate and Multivariate Cox Regression Analyses of Clinical Factors Associated with Recurrence in Targeted Therapy Patients with HCC

Characteristic	Univariate HR (95% CI)	*P*	Multivariate HR (95% CI)	*P*
Surgery	0.602 (0.470–0.771)	**<0.001**	0.527 (0.405–0.685)	**<0.001**
NT	1.306 (1.041–1.640)	**0.021**		
Pre-MDT	1.231 (0.986–1.537)	0.067		
Satellite nodules	1.017 (0.825–1.255)	0.872		
Degree of differentiation	1.173 (0.938–1.467)	0.161		
MVI	1.218 (0.976–1.521)	0.081		
MDT	1.836 (1.462–2.306)	**<0.001**	2.079 (1.624–2.662)	**<0.001**
AFP	1.247 (1.006–1.546)	**0.044**	1.307 (1.041–1.641)	**0.021**
GGT	0.952 (0.762–1.190)	0.667		
HBV	1.127 (0.899–1.412)	0.299		
Nerve invasion	0.968 (0.770–1.217)	0.779		
Bile duct invasion and cancer thrombus	1.167 (0.944–1.443)	0.154		
ALP	1.291 (1.070–1.557)	**0.008**		
Pre-AFP	0.990 (0.789–1.242)	0.932		
Invention	1.029 (0.818–1.294)	0.809		
EOS	1.106 (0.887–1.379)	0.372		
Pre-Intervention	0.787 (0.628–0.987)	**0.038**	0.748 (0.590–0.949)	**0.017**
PLR	0.953 (0.743–1.221)	0.703		
Liver capsule	1.020 (0.820–1.269)	0.860		
PLT	1.025 (0.824–1.275)	0.827		
HGB	0.887 (0.696–1.132)	0.336		
Pre-NT	0.874 (0.686–1.114)	0.278		
First recurrence site	1.113 (0.882–1.406)	0.366		
NER	0.957 (0.777–1.178)	0.676		
LMR	0.866 (0.691–1.087)	0.215		
Age at surgery	1.286 (1.032–1.602)	**0.025**	1.354 (1.079–1.699)	**0.009**
NLR	1.032 (0.849–1.255)	0.750		
DBIL	0.727 (0.360–1.468)	0.373		
AST	1.055 (0.862–1.291)	0.605		
LYM	1.039 (0.816–1.322)	0.758		
ALB	0.972 (0.790–1.196)	0.791		
TBIL	0.683 (0.371–1.259)	0.222		
MONO	1.158 (0.936–1.433)	0.177		
Gender	1.093 (0.854–1.398)	0.479		
IBIL	0.793 (0.592–1.062)	0.120	0.664 (0.471–0.937)	**0.020**
RBC	0.925 (0.734–1.167)	0.512		
Cirrhosis	0.911 (0.731–1.136)	0.408		
NEU	1.130 (0.917–1.392)	0.253		
BASO	0.973 (0.836–1.131)	0.719		
ALT	1.018 (0.810–1.279)	0.879		
WBC	1.141 (0.917–1.419)	0.238		
TKI-ICI therapy	0.967 (0.771–1.212)	0.769		

Notes: Bold values indicate statistically significant differences (***P*** < 0.05).

Abbreviations: NT, number of tumors; Pre-MDT, preoperative maximum tumor diameter; MVI, microvascular invasion; MDT, maximum tumor diameter; AFP, alpha-fetoprotein; GGT, gamma-glutamyl transferase; HBV, hepatitis B virus; ALP, alkaline phosphatase; Pre-AFP, preoperative alpha-fetoprotein; EOS, eosinophil count; Pre-intervention, preoperative intervention; PLR, platelet-to-lymphocyte ratio; PLT, platelet count; HGB, hemoglobin; Pre-NT, preoperative number of tumors; NER, neutrophil-to-erythrocyte ratio; LMR, lymphocyte-to-monocyte ratio; NLR, neutrophil-to-lymphocyte ratio; DBIL, direct bilirubin; AST, aspartate aminotransferase; LYM, lymphocyte count; ALB, albumin; TBIL, total bilirubin; MONO, monocyte count; IBIL, indirect bilirubin; RBC, red blood cell count; NEU, neutrophil count; BASO, basophil count; ALT, alanine aminotransferase; WBC, white blood cell count; TKI-ICI therapy, tyrosine kinase inhibitor and immune checkpoint inhibitor therapy.

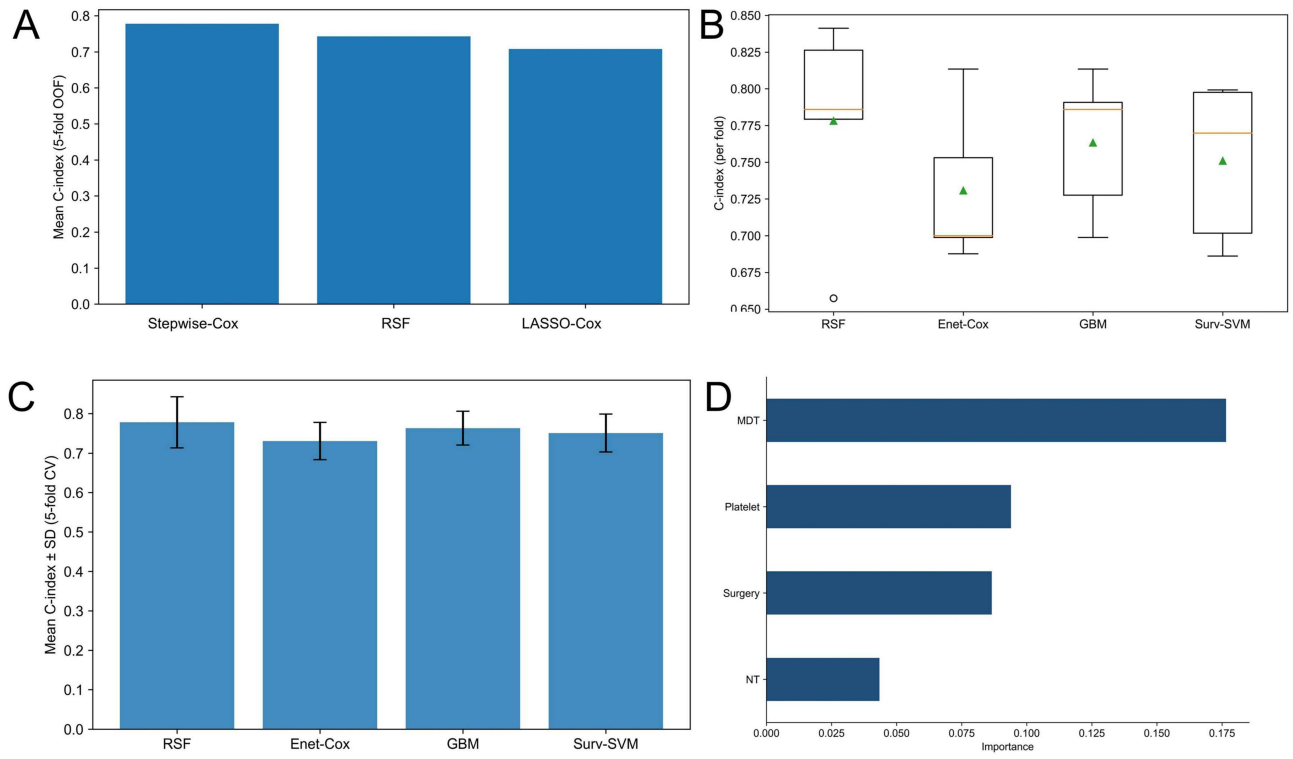

Figure 5 Development and evaluation of the prognostic prediction model for the TKI therapy cohort. (**A**) Comparison of three feature selection methods: stepwise Cox regression, random survival forest (RSF), and LASSO-Cox regression. (**B**) Distribution of the concordance index (C-index) across five-fold cross-validation for the four candidate prediction algorithms. (**C**) Performance comparison of the four machine learning algorithms based on comprehensive evaluation metrics. (**D**) Ranking of the importance of the selected predictive features in the final model.

Model Validation and Evaluation

The RSF model effectively stratified patients into high- and low-risk groups (training C-index = 0.856, validation C-index = 0.838, both $P < 0.001$; Figure 6A and B). Predictive performance remained stable within 48 months (Figure 6C). Time-dependent Brier scores stabilized between 0.48–0.49 (Figure 6D), and the 24-month calibration curve demonstrated good accuracy (Figure 6E and F). SHAP analysis (Figure 6G) confirmed maximum tumor diameter at recurrence as the primary risk factor and surgery/ablation after recurrence as a key protective factor.

Treatment Strategy Matching Analysis Based on Counterfactual Predictions

Using the two validated models, counterfactual analysis of the entire cohort (n = 454) yielded the following strategy matching: 213 patients (46.9%) were aligned with the model's recommendation for non-TKI therapy; 135 patients (29.7%) were aligned for TKI therapy; 94 patients (20.7%) receiving non-TKI therapy were recommended to switch to TKI therapy; and 12 patients (2.6%) receiving TKI therapy were recommended to switch to non-TKI therapy. Overall, 348 patients (76.6%) were in the "treatment-concordant" group, whereas 106 patients (23.4%) comprised the "potential treatment-mismatch" group (Figure 7).

Discussion

The optimal management of HCC recurrence after curative resection remains insufficiently defined, largely due to the lack of high-level evidence guiding post-recurrence treatment selection. Although TKIs are widely used in advanced HCC, their survival benefit in the post-resection recurrent setting remains controversial.[13] In this study, by applying overlap weighting based on propensity scores to minimize confounding, we demonstrated that TKI therapy was associated with significantly improved recurrence-free survival (HR = 0.355) and overall survival (HR = 0.486) compared with non-TKI therapy. These findings provide robust real-world evidence supporting the effectiveness of TKI therapy in patients with recurrent HCC after curative resection.[6]

https://doi.org/10.2147/JHC.S599142

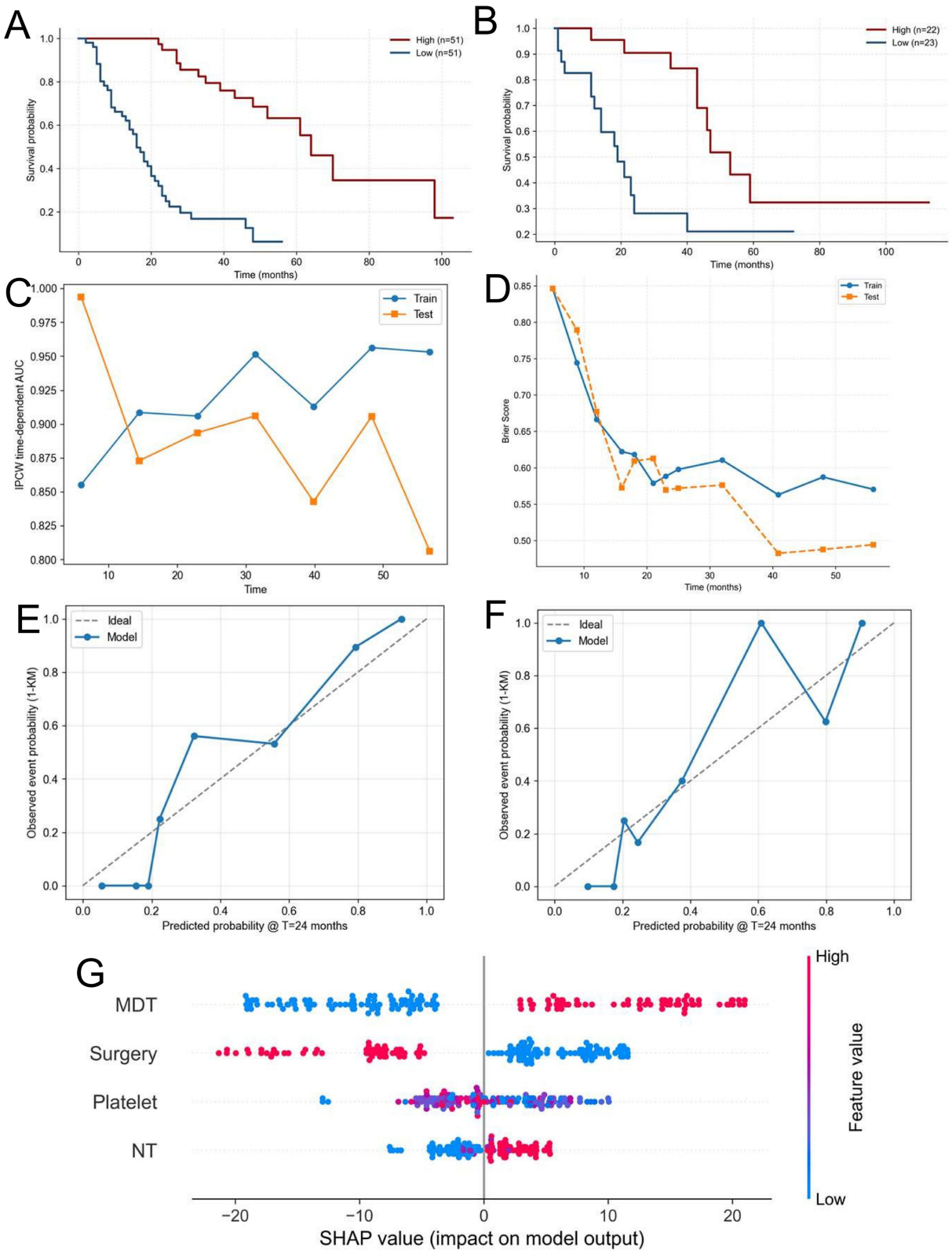

Figure 6 Validation and interpretation of the prognostic model for the TKI therapy cohort. (**A**) Kaplan-Meier overall survival (OS) curves for the low- and high-risk groups in the training set. (**B**) Kaplan-Meier overall survival (OS) curves for the low- and high-risk groups in the validation set. (**C**) Time-dependent area under the curve (AUC) for the model over the 48-month follow-up period. (**D**) Time-dependent Brier score for assessing the calibration of the model. (**E** and **F**) Calibration plots comparing predicted and observed survival probability at 24 months. (**G**) SHapley Additive exPlanations (SHAP) summary plot showing the impact of key features on model output.

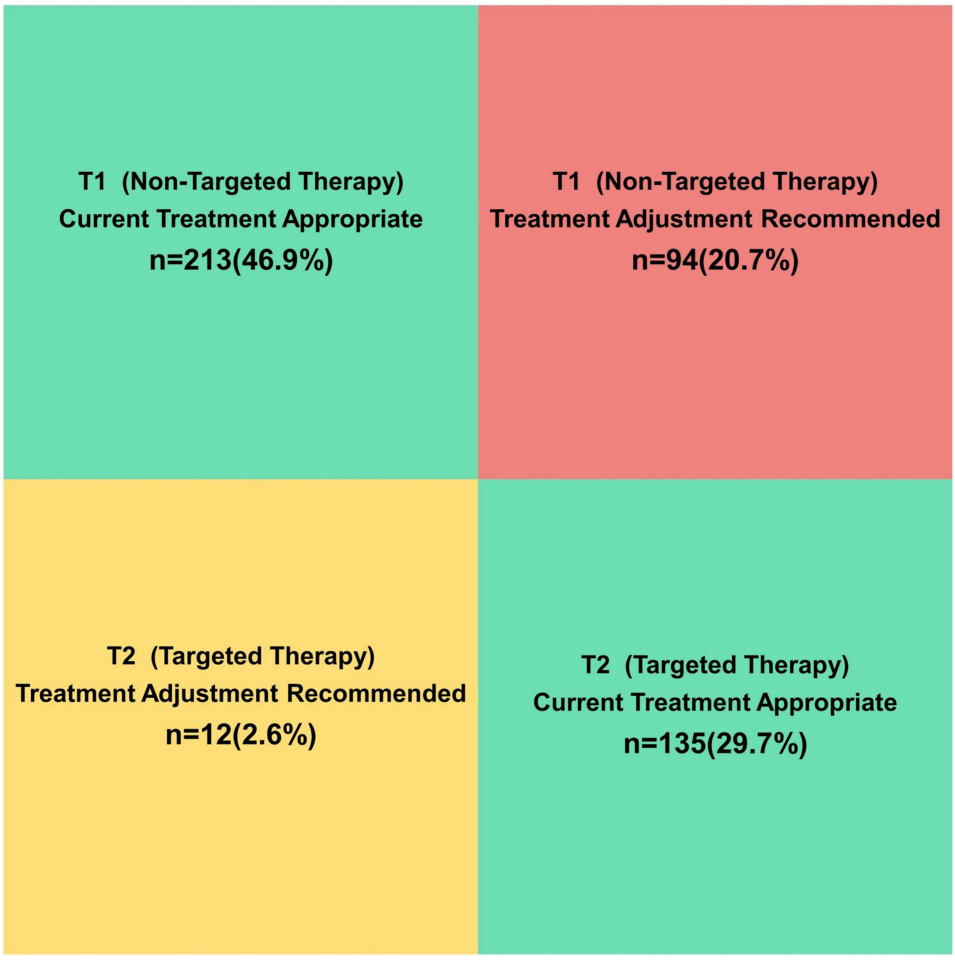

Figure 7 Distribution of treatment strategy alignment following counterfactual analysis.The chart categorizes patients into four groups based on the comparison of their actual treatment and the optimal treatment predicted by the validated models.

Beyond confirming population-level treatment benefit, an important strength of this study lies in its focus on individualized therapeutic decision-making. Recognizing the marked heterogeneity in recurrent HCC, we developed separate machine learning–based prognostic models for TKI-treated and non-TKI-treated patients. By integrating these treatment-specific models within a counterfactual inference framework, we were able to quantify individualized survival outcomes under alternative treatment scenarios. This dual-scenario modeling approach moves beyond traditional risk stratification and enables personalized estimation of treatment benefit, thereby facilitating data-driven optimization of post-recurrence treatment strategies for patients with HCC.

The treatment-specific models revealed distinct prognostic architectures. In the TKI-treated cohort, key predictors emphasized the dominant roles of tumor burden and the immune–inflammatory milieu. Maximum tumor diameter at recurrence emerged as the most influential risk factor, consistent with prior evidence indicating that baseline tumor size critically affects responsiveness to TKIs such as sorafenib and lenvatinib.[14] Larger recurrent tumors may reflect greater intratumoral heterogeneity and a more complex tumor microenvironment, thereby attenuating the therapeutic efficacy of angiogenesis- and signaling pathway–targeted agents. The inclusion of platelet count further underscores its dual significance as an indicator of hepatic functional reserve and an active mediator of systemic inflammation and tumor progression. Platelets have been shown to facilitate angiogenesis, immune evasion, and metastatic niche formation through the release of pro-angiogenic and immunomodulatory factors, mechanisms that may directly or indirectly modulate sensitivity to TKI therapy.[15,16] Notably, the TKI-specific model incorporated fewer prognostic features overall. This observation may reflect a relative "simplification" of disease progression pathways once key oncogenic signaling

https://doi.org/10.2147/JHC.S599142

axes (eg., VEGFR and FGFR) are pharmacologically inhibited. Under such conditions, patient prognosis may become more strongly determined by the agent's capacity to control dominant tumor burden characteristics and by the host's ability to sustain an immune microenvironment conducive to effective treatment response.[17]

Conversely, the prognostic model for the non-TKI cohort incorporated a broader array of variables, reflecting the multifactorial nature of disease progression in the absence of targeted intervention. In addition to number of recurrent tumors, a well-established surrogate for intrahepatic dissemination and multicentric recurrence,[18] the model retained primary tumor pathological features, underscoring the persistent influence of intrinsic tumor biology on post-recurrence outcomes. The inclusion of alpha-fetoprotein level at recurrence further highlights its role as a canonical biomarker of tumor aggressiveness and proliferative activity, as well as a predictor of therapeutic responsiveness in advanced HCC.[19] Importantly, HBV infection status emerged as a clinically relevant determinant, consistent with evidence that effective antiviral therapy confers a survival advantage in virus-related HCC following curative resection.[20] Ongoing viral replication and the associated chronic inflammatory milieu may accelerate hepatocarcinogenesis and promote tumor progression when systemic anticancer therapy is absent. Taken together, the differential feature composition between the two models suggests that, without TKI treatment, patient prognosis is more heavily governed by the tumor's inherent invasive potential and the host's sustained inflammatory state, whereas TKI therapy may partially override these drivers by constraining key oncogenic signaling pathways.

In summary, although the independent prognostic factors selected by the two models demonstrated both overlap and divergence, one shared finding carries particularly important clinical implications. The therapeutic paradigm of systemic therapy combined with local treatment constitutes the cornerstone of management for advanced hepatocellular carcinoma and is consistently recommended by major international guidelines.[21–23]Recent evidence further indicates that integrated locoregional and systemic strategies can improve survival outcomes in patients with recurrent hepatocellular carcinoma by synergistically controlling macroscopic disease and modulating the tumor microenvironment.[24] In the present study, receipt of radical local treatment (surgical resection or ablation) after recurrence emerged as the most influential protective factor in both subgroup-specific models. This consistent finding strongly suggests that the principle of combining systemic therapy with aggressive local control remains applicable—and prognostically advantageous—even in patients who experience recurrence following curative resection. These results are in line with contemporary retrospective analyses demonstrating that surgical or ablative control of recurrent lesions is independently associated with prolonged overall survival and delayed disease progression in recurrent HCC.[25] Importantly, this observation underscores that, irrespective of the subsequent systemic treatment strategy, effective eradication of macroscopic recurrent lesions represents a universal foundation for improving post-recurrence outcomes.

The principal distinction between the two models lies in the composition and complexity of their feature sets. The TKI-treated model was comparatively parsimonious, potentially reflecting a "simplification" of dominant prognostic drivers under TKI therapy, with outcomes being governed primarily by residual tumor burden and the host immune microenvironment. In contrast, the non-TKI model captured a broader spectrum of variables, more comprehensively characterizing the tumor's intrinsic invasive behavior and the patient's chronic inflammatory state in the absence of targeted oncogenic pathway inhibition. This divergence is consistent with emerging evidence suggesting that targeted systemic therapies may partially override tumor-intrinsic heterogeneity by suppressing key oncogenic signaling pathways, thereby reshaping the prognostic landscape.[26] This critical divergence highlights the methodological and clinical value of our treatment-stratified modeling strategy, suggesting that a single unified prognostic model may be insufficient to accurately reflect the heterogeneous biological mechanisms influencing prognosis across different therapeutic pathways.[27]

The central advancement of our framework lies in its transition from conventional prognostic estimation to clinically actionable decision support. This innovation is supported by two key strengths. First, model development and reporting rigorously adhered to international standards for clinical prediction research, ensuring methodological transparency, robustness, and reproducibility.[28] Moreover, all predictive variables were derived from routinely available clinical data, obviating the need for specialized or costly testing and thereby enhancing the feasibility of real-world implementation. Second, and most notably, this study pioneers a dual-scenario modeling strategy integrated with counterfactual reasoning.[29] Consistent with prior applications of counterfactual frameworks in clinical research,[12,30] this approach

enables estimation of individualized survival outcomes under alternative treatment strategies, allowing objective identification of potential treatment mismatch at the patient level. Consequently, our treatment-matching simulation revealed that approximately 23.4% of patients within the cohort may derive substantial benefit from optimization of their current therapeutic strategy.

Several recent studies have developed radiomics and deep learning models to predict HCC recurrence or treatment response. Ren et al applied CT-based machine learning to predict outcomes in HCC patients receiving TACE plus TKI therapy;[31] Wang et al integrated MR radiomics with deep learning to predict post-ablation recurrence;[32] Liu et al constructed a pathology-based deep learning model for postoperative recurrence risk and sorafenib response;[33] Chen et al combined conventional radiomics and deep learning features to predict early recurrence after curative ablation.[34] While bioinformatics approaches have been employed to identify hub genes and predictive signatures for HCC treatment response.[35] These studies collectively demonstrate the potential of artificial intelligence to personalize HCC management. Compared with these approaches, our model offers distinct advantages: it directly compares survival outcomes between TKI and non-TKI therapies in the specific setting of postoperative recurrence, and provides individualized treatment benefit estimates through a counterfactual framework. Moreover, our model relies solely on routinely available clinical and laboratory variables, making it more readily generalizable across institutions without requiring specialized imaging or pathology pipelines. However, a trade-off exists: our model may not capture tumor morphological heterogeneity as effectively as image-based deep learning models. Therefore, the two approaches are complementary. Future work could integrate clinical variables with radiomics and pathological features to further improve predictive accuracy for post-recurrence TKI benefit.

This study has several limitations. First, as a single-center retrospective analysis, residual or unmeasured confounding cannot be fully excluded, despite the use of advanced overlap weighting based on propensity scores to mitigate measured confounders. Second, the TKI-treated group included both sorafenib and lenvatinib without agent-specific subgroup analysis due to limited sample size, precluding assessment of differential survival benefits between individual TKIs. Moreover, because the TKI and non-TKI models were trained on separate subgroups with potentially different feature distributions, applying a patient's baseline characteristics to both models may introduce prediction errors for underrepresented profiles; thus, individualized treatment benefit estimates should be interpreted with caution. Third, our models focus solely on survival outcomes and do not incorporate treatment toxicity, cost, patient preferences, or quality of life, which are critical for clinical decision-making. Finally, although the models demonstrated robust internal validation and favorable performance, their generalizability remains to be established through external validation. Future research should include prospective, multi-center data collection to assess the real-world clinical utility and further refine the treatment-matching framework.

Conclusion

This study demonstrates that tyrosine kinase inhibitor therapy provides a significant survival benefit in patients with postoperative recurrent hepatocellular carcinoma, as shown through rigorous propensity score-based adjustment. By integrating machine learning-based prognostic models with counterfactual inference, we enable individualized estimation of treatment benefit and predictive survival outcomes. This framework represents a step toward data-driven, precision management of recurrent HCC and may inform personalized post-recurrence therapeutic decisions. Prospective validation and evaluation of clinical implementation are warranted before routine application.

Abbreviations

HCC, hepatocellular carcinoma; TKI, tyrosine kinase inhibitor; HBV, hepatitis B virus; NLR, neutrophil-to-lymphocyte ratio; PLR, platelet-to-lymphocyte ratio; LMR, lymphocyte-to-monocyte ratio; OS, overall survival; RFS, recurrence-free survival; SMDs, standardized mean differences; C-index, concordance index; RSF, random survival forest; GBM, gradient boosting machine; Surv-SVM, Survival support vector machine; AUC, area under the curve; SHAP, the Shapley additive explanations.

Data Sharing Statement

The data supporting the findings of this study are available from the corresponding author upon reasonable request (Jingyu Cao, E-mail cjy7027@163.com).

Ethics Approval and Consent to Participate

The protocol of this study was approved by the ethical review board of the Affiliated Hospital of Qingdao University (No. QYFY-WZLL-42256).

Acknowledgments

Thank all the staff authors for their contributions to this study.

Author Contributions

All authors made a significant contribution to the work reported, whether that is in the conception, study design, execution, acquisition of data, analysis and interpretation, or in all these areas; took part in drafting, revising or critically reviewing the article; gave final approval of the version to be published; have agreed on the journal to which the article has been submitted; and agree to be accountable for all aspects of the work.

Funding

This study was supported by the Taishan Scholar Foundation of Shandong Province, the Shandong Provincial Natural Science Foundation (ZR2024QH265 and ZR2025MS1290), the Shandong Provincial Medical and Health Science and Technology Development Plan (202425020784), the Shandong Higher Education Young Science and Technology Support Program (2024KJJ041), the Qingdao Natural Science Foundation (24-4-4-zrjj-103-jch), and the Medical and Health Scientific Research Project of Qingdao (2024-WJKY173).

Disclosure

All authors declare no competing interests.

References

1. Siegel RL, Giaquinto AN, Jemal A. Cancer statistics, 2024. *CA Cancer J Clin*. 2024;74(1):12–49. doi:10.3322/caac.21820
2. Llovet JM, Kelley RK, Villanueva A, et al. Hepatocellular carcinoma. *Nat Rev Dis Primer*. 2021;7(1):6. doi:10.1038/s41572-020-00240-3
3. Sensi B, Angelico R, Toti L, et al. Mechanism, potential, and concerns of immunotherapy for hepatocellular carcinoma and liver transplantation. *Curr Mol Pharmacol*. 2024;17:e1012161775. doi:10.2174/0118761429310703240823045808
4. Finn RS, Qin S, Ikeda M, et al. Atezolizumab plus bevacizumab in unresectable hepatocellular carcinoma. *New Engl J Med*. 2020;382(20):1894–1905. doi:10.1056/NEJMoa1915745
5. Ren Z, Xu J, Bai Y, et al. Sintilimab plus a bevacizumab biosimilar (ibi305) versus sorafenib in unresectable hepatocellular carcinoma (orient-32): a randomised, open-label, Phase 2–3 study. *Lancet Oncol*. 2021;22(7):977–990. doi:10.1016/S1470-2045(21)00252-7
6. Li J, Wang W, Zhu R, et al. Postoperative adjuvant tyrosine kinase inhibitors combined with anti-pd-1 antibodies improves surgical outcomes for hepatocellular carcinoma with high-risk recurrent factors. *Front Immunol*. 2023;14:1202039. doi:10.3389/fimmu.2023.1202039
7. Payo-Serafín T, Méndez-Blanco C, Fernández-Palanca P, et al. Risk versus benefit of tyrosine kinase inhibitors for hepatocellular carcinoma: a systematic review and meta-analysis of randomized controlled trials. *Clin Pharmacol Ther*. 2024;116(2):328–345. doi:10.1002/cpt.3312
8. Haak F, Di Tommaso L, Viganò L, et al. A transcriptomic signature of intrahepatic cholangiocellular carcinoma with very early recurrence: identifying patients at risk and finding a personalized adjuvant therapy. *Eur J Surg Oncol*. 2023;49(2):e214. doi:10.1016/j.ejso.2022.11.586
9. Sun B, Chen L, Lei Y, et al. Sorafenib plus transcatheter arterial chemoembolization with or without camrelizumab for the treatment of intermediate and advanced hepatocellular carcinoma. *Br J Radiol*. 2024;97(1159):1320–1327. doi:10.1093/bjr/tqae087
10. Xu W, Liao S, Hu Y, Huang Y, Zhou J. Upregulation of mir-3130-5p enhances hepatocellular carcinoma growth by suppressing ferredoxin 1: mir-3130-5p enhances hcc growth via inhibiting fdx1. *Curr Mol Pharmacol*. 2024;17:e1012209080. doi:10.2174/0118761429358008250305070518
11. Ye W, Wang J, Zheng J, Jiang M, Zhou Y, Wu Z. Association between higher expression of vav1 in hepatocellular carcinoma and unfavourable clinicopathological features and prognosis. *Protein Pept Lett*. 2024;31(9):706–713. doi:10.2174/0109298665330781240830042601
12. Famularo S, Donadon M, Cipriani F, et al. Machine learning predictive model to guide treatment allocation for recurrent hepatocellular carcinoma after surgery. *JAMA Surg*. 2023;158(2):192–202. doi:10.1001/jamasurg.2022.6697
13. Wang Z, Fan J, Zhou S, et al. Perioperative camrelizumab plus rivoceranib versus surgery alone in patients with resectable hepatocellular carcinoma at intermediate or high risk of recurrence (cares-009): a randomised phase 2/3 trial. *Lancet*. 2025;406(10515):2089–2099. doi:10.1016/S0140-6736(25)01720-9

14. Llovet JM, Montal R, Sia D, Finn RS. Molecular therapies and precision medicine for hepatocellular carcinoma. *Nat Rev Clin Oncol*. 2018;15(10):599–616. doi:10.1038/s41571-018-0073-4
15. Tian X, Liu X, Zeng F, Chen Z, Wu D. Platelet-to-lymphocyte ratio acts as an independent risk factor for patients with hepatitis b virus-related hepatocellular carcinoma who received transarterial chemoembolization. *Eur Rev Med Pharmacol*. 2016;20(11):2302.
16. Sierko E, Wojtukiewicz MZ. Platelets and angiogenesis in malignancy. *Semin Thromb Hemost*. 2004;30(1):95–108. doi:10.1055/s-2004-822974
17. Sia D, Villanueva A, Friedman SL, Llovet JM. Liver cancer cell of origin, molecular class, and effects on?patient prognosis. *Gastroenterology*. 2017;152(4):745–761. doi:10.1053/j.gastro.2016.11.048
18. Zeng J, Zeng J, Lin K, et al. Development of a machine learning model to predict early recurrence for hepatocellular carcinoma after curative resection. *Hepatobil Surg Nutr*. 2022;11(2):176–187. doi:10.21037/hbsn-20-466
19. Personeni N, Bozzarelli S, Pressiani T, et al. Usefulness of alpha-fetoprotein response in patients treated with sorafenib for advanced hepatocellular carcinoma. *J Hepatol*. 2012;57(1):101–107. doi:10.1016/j.jhep.2012.02.016
20. Huang DQ, Hoang JK, Kamal R, et al. Antiviral therapy utilization and 10-year outcomes in resected hepatitis b virus- and hepatitis c virus-related hepatocellular carcinoma. *J Clin Oncol*. 2024;42(7):790–799. doi:10.1200/JCO.23.00757
21. Reig M, Forner A, Rimola J, et al. BCLC strategy for prognosis prediction and treatment recommendation: the 2022 update. *J Hepatol*. 2022;76(3):681–693. doi:10.1016/j.jhep.2021.11.018
22. European AFTS. EASL clinical practice guidelines on the management of hepatocellular carcinoma. *J Hepatol*. 2025;82(2):315–374. doi:10.1016/j.jhep.2024.08.028
23. Heimbach JK, Kulik LM, Finn RS, et al. Aasld guidelines for the treatment of hepatocellular carcinoma. *Hepatology*. 2018;67(1):358–380. doi:10.1002/hep.29086
24. Liang J, Bai Y, Ha F, Luo Y, Deng H, Gao Y. Combining local regional therapy and systemic therapy: expected changes in the treatment landscape of recurrent hepatocellular carcinoma. *World J Gastro Oncol*. 2023;15(1):1–18. doi:10.4251/wjgo.v15.i1.1
25. Ohama H, Hiraoka A, Tada F, et al. Clinical usefulness of surgical resection including the complementary use of radiofrequency ablation for intermediate-stage hepatocellular carcinoma. *Cancers*. 2022;15(1):236. doi:10.3390/cancers15010236
26. Li L, Li Z, Pan L, et al. Adjuvant therapy for hepatocellular carcinoma after curative treatment: several unanswered questions. *J Clin Transl Hepatol*. 2024;12(5):525–533. doi:10.14218/JCTH.2024.00030
27. Kent DM, van Klaveren D, Paulus JK, et al. The predictive approaches to treatment effect heterogeneity (path) statement: explanation and elaboration. *Ann Intern Med*. 2020;172(1):W1–W25. doi:10.7326/M18-3668
28. Collins GS, Reitsma JB, Altman DG, Moons KGM. Transparent reporting of a multivariable prediction model for individual prognosis or diagnosis (tripod). *Ann Intern Med*. 2015;162(10):735–736. doi:10.7326/L15-5093-2
29. Wei X, Wang F, Liu Y, et al. A machine learning model based on counterfactual theory for treatment decision of hepatocellular carcinoma patients. *J Hepatocell Carcinoma*. 2024;11:1675–1687. doi:10.2147/JHC.S470550
30. Li X, Liang X, Chen S, et al. Development and validation of a ct-based online calculator for prognosis and postoperative adjuvant transcatheter arterial chemoembolization benefit prediction in resected hepatocellular carcinoma: a multicenter retrospective cohort study. *Int J Surg*. 2025;2025:10–1097. doi:10.1097/JS9.0000000000004456.
31. Ren Q, Zhu P, Li C, et al. Pretreatment computed tomography-based machine learning models to predict outcomes in hepatocellular carcinoma patients who received combined treatment of trans-arterial chemoembolization and tyrosine kinase inhibitor. *Front Bioeng Biotechnol*. 2022;10:872044. doi:10.3389/fbioe.2022.872044
32. Wang Y, Zhang Y, Xiao J, Geng X, Han L, Luo J. Multicenter integration of mr radiomics, deep learning, and clinical indicators for predicting hepatocellular carcinoma recurrence after thermal ablation. *J Hepatocell Carcinoma*. 2024;11:1861–1874. doi:10.2147/JHC.S482760
33. Li Y, Xiong J, Hu Z, et al. Denoised recurrence label-based deep learning for prediction of postoperative recurrence risk and sorafenib response in hcc. *Bmc Med*. 2025;23(1):162. doi:10.1186/s12916-025-03977-4
34. Li Y, Qian G, Zhu Y, et al. An integrated model combined conventional radiomics and deep learning features to predict early recurrence of hepatocellular carcinoma eligible for curative ablation: a multicenter cohort study. *J Comput Assist Tomo*. 2025;49(6):860–871. doi:10.1097/RCT.0000000000001764
35. Gudivada IP, Amajala KC. Integrative bioinformatics analysis for targeting hub genes in hepatocellular carcinoma treatment. *Curr Genomics*. 2025;26(1):48–80. doi:10.2174/0113892029308243240709073945